

# Numerical mode matching in dissipative silencers with temperature gradients and mean flow

Eva M. Sánchez-Orgaz, Francisco D. Denia, Luis Baeza

Centro de Investigación de Tecnología de Vehículos, Universitat Politècnica de València, Valencia, Spain.

Ray Kirby

School of Engineering and Design, Mechanical Engineering, Brunel University, Uxbridge, Middlesex, United Kingdom.

## Summary

This work presents a mathematical approach based on the mode matching method to compute the transmission loss of perforated dissipative silencers with temperature gradients and mean flow. Three-dimensional wave propagation is considered in silencer geometries with arbitrary, but axially uniform, cross section. To reduce the computational requirements of a full multidimensional finite element calculation, a method is developed combining axial and transversal solutions of the wave equation. First, the finite element method is employed in a two-dimensional problem to extract the eigenvalues and associated eigenvectors for the silencer cross section. Mean flow as well as radial temperature gradients and the corresponding thermal-induced material heterogeneities are included in the model. Assuming a low acoustic influence of axial gradients (compared to radial variations), an axially uniform temperature field is taken into account, its value being the inlet/outlet average. A weighted residual approach is then used to match the acoustic fields (pressure and axial acoustic velocity) at the geometric discontinuities between the silencer chamber and the inlet and outlet pipes. Transmission loss predictions are compared favourably with a general three-dimensional finite element approach, offering a reduction in the computational effort.

PACS no. 43.50.Gf, 43.20.Mv

## 1. Introduction

Dissipative silencers have been widely used in automotive applications due to their efficiency in the mid and high frequency range. A review of the bibliography published during the last years shows the rise of multidimensional techniques [1-7] to characterize the acoustic behaviour of silencers in comparison with one-dimensional techniques, due to their higher accuracy in the silencer operating frequency range. Between the multidimensional techniques, the finite element method (FEM) presents versatility when the silencer has a complex geometry [4, 5] or when more realistic operating conditions are considered, such as the presence of mean flow and heterogeneous properties of the dissipative material [8, 9] or temperature variations [10]. However, these numerical techniques have the disadvantage of being computationally expensive when a high

number of degrees of freedom is considered. In order to avoid this problem in silencers with arbitrary (but axially uniform) cross section, Kirby [4, 6] obtained the axial wavenumbers and pressure modes associated with the silencer cross section using a two-dimensional FE model. This eigensolution was then combined with the point collocation method [4] and, in a later work, with the mode-matching technique [6], to obtain the wave amplitudes corresponding to the waves of the different silencer regions, the continuity conditions of the pressure and axial acoustic velocity being taken into account. Although these approaches deliver a considerable reduction in the computational effort, attention has to be paid to some numerical issues, as those found in the point collocation approach [4, 11, 12] where predictions exhibit a high sensitivity to silencer geometry and also the collocation grid.

The temperature variation within the silencer can reach, in some configurations, values around 200°C in the axial direction [13] and more than 100°C in the radial one [14]. The temperature distribution can affect the acoustic behaviour of the silencer considerably. Several authors studied the influence of these gradients in the silencer transmission loss. Kim *et al.* [15] applied an analytic multidimensional approach to some reactive configurations considering axial temperature variation and mean flow. In this work, to model the acoustic effect of the temperature gradient, the silencer was divided into segments of uniform temperature, obtaining the acoustic fields in each segment by using the corresponding continuity conditions. Wang *et al.* [16] combined a segmentation procedure with the boundary element method (BEM) considering uniform mean flow and linear axial temperature gradients. Denia *et al.* [10] considered both axial and radial gradients in a dissipative configuration in the presence of mean flow. As it was shown in this work, the impact of axial thermal variations on the acoustic behaviour of dissipative silencers is not as relevant as the radial distribution; this is the reason why the current investigation only retains transversal thermal gradients while an axially uniform temperature is assumed in both the central duct and the chamber, its value being the average temperature of the inlet and the outlet sections. Since the radial temperature gradients can have a considerable influence on the silencer noise attenuation [10], these gradients have been considered in the present work by means of an approach that allows the consideration of non-homogeneous properties in the cross section. As temperature gradients have an effect on the acoustic properties of the propagation medium [10, 17-19], and consequently the acoustic impedance of the perforated surface is also affected [20-23], the techniques used to characterize the silencers have been numerical in general, due to the complexity of the computations required. This fact supposes a high computational cost, and to avoid this drawback, in the present work an extension of the approach proposed by Kirby [6] is presented and applied to a silencer with heterogeneous properties over the cross section. A 2D acoustic problem modelled with the FEM is combined with the mode matching technique, allowing the acoustic characterization of dissipative silencers with arbitrary cross section, including transversal thermal gradients and mean flow. The approach yields a computationally efficient modelling tool.

## 2. Formulation of the acoustic problem and mathematical approach

The geometry of the configuration under study (with uniform but arbitrary cross section) appears in Figure 1. The silencer consists of a perforated central duct carrying mean flow, which is surrounded by an outer chamber (of length  $L_c$ ) containing absorbent material. In the chamber the temperature presents transversal variations, while axial uniformity is assumed, with a constant value computed as the average of the temperature at the inlet and outlet sections. The absorbent material and air regions are denoted as  $\Omega_m$  and  $\Omega_a$ , respectively, while its boundary surfaces are  $\Gamma_m$  and  $\Gamma_a$ . Within the perforated surface  $\Gamma_p$  the propagation medium is air, its relevant properties being the density  $\rho_0$  the velocity of sound  $c_0$ . In  $\Omega_m$  the equivalent properties of the absorbent material are denoted as  $\rho_m(x, y)$  and  $c_m(x, y)$ , both being complex, frequency-dependent as well as coordinate-dependent. The inlet and outlet pipes are equal and have a uniform circular cross section (denoted as 1 and 3 respectively).

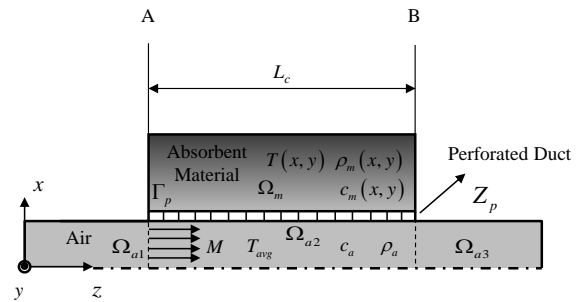


Figure 1. Geometry of the silencer.

First, the computation of the eigenvalues (wavenumbers) and eigenfunctions (pressure modes) corresponding to each section (inlet/outlet pipes and chamber) is required [4, 6]. As the evaluation of the eigenvalues and the eigenfunctions associated with the inlet/outlet pipes is straightforward, only the eigenvalue problem related to the chamber is presented. After that, the pressure and axial acoustic velocity continuity conditions will be combined with a numerical mode matching scheme to obtain the complete solution of the acoustic field inside the silencer and its acoustic attenuation performance through the transmission loss [6].

### 2.1. Acoustic equations

The sound propagation in the air, assuming harmonic behaviour, is governed by [1, 4]

$$\frac{\partial^2 p_{a2}}{\partial x^2} + \frac{\partial^2 p_{a2}}{\partial y^2} + (1-M^2) \frac{\partial^2 p_{a2}}{\partial z^2} - 2jMk_0 \frac{\partial p_{a2}}{\partial z} + k_0^2 p_{a2} = 0 \quad , (1)$$

$p_{a2}$  being the complex amplitude of the acoustic pressure and  $k_0 = \omega / c_0$  the wavenumber (where  $\omega$  is the angular frequency). The wave equation in the absorbent material can be written as [9]

$$\nabla \left( \frac{1}{\rho_m} \nabla p_m \right) + \frac{1}{\rho_m} k_m^2 p_m = 0 \quad , (2)$$

$p_m$  being the acoustic pressure amplitude and  $k_m = \omega / c_m$  the wavenumber associated with the absorbent material.

The cross section is uniform and, therefore, application of the method of separation of variables yields

$$p_{a2}(x, y, z) = \Psi^{xy}(x, y) e^{-jk_z z}$$

$$\Psi^{xy}(x, y) = \begin{cases} \Psi_{a2}^{xy}(x, y), & (x, y) \in \Omega_a \\ \Psi_m^{xy}(x, y), & (x, y) \in \Omega_m \end{cases} \quad , (3)$$

where  $\Psi^{xy}$  is the transversal pressure mode and  $k_z$  is the axial wavenumber. Now, combining equations (3) with (1) and (2) provides

$$\nabla^2 \Psi_a^{xy} + (k_0^2 - 2Mk_0 k_z - (1-M^2)k_z^2) \Psi_a^{xy} = 0 \quad , (4)$$

$$\nabla \left( \frac{1}{\rho_m} \nabla \Psi_m^{xy} \right) + \frac{1}{\rho_m} (k_m^2 - k_z^2) \Psi_m^{xy} = 0 \quad , (5)$$

where subscript 2 in the air has been omitted for simplicity.

## 2.2. FEM approach and eigenvalue problem

At the silencer cross section, the acoustic pressure can be approximated by using trial functions as follows [24]

$$\Psi_a^{xy}(x, y) = \sum_{i=1}^{N_a} N_{a_i}^{xy}(x, y) \Psi_{a_i} = \mathbf{N}_a^T \boldsymbol{\Psi}_a, \quad (x, y) \in \Omega_a \quad , (6)$$

$$\Psi_m^{xy}(x, y) = \sum_{i=1}^{N_m} N_{m_i}^{xy}(x, y) \Psi_{m_i} = \mathbf{N}_m^T \boldsymbol{\Psi}_m, \quad (x, y) \in \Omega_m \quad , (7)$$

where the subscripts  $a$  and  $m$  correspond to the air and absorbent material regions, respectively. In general,  $N(x, y)$  is a global shape function,  $\mathbf{N}_a$  and  $\mathbf{N}_m$  contain the nodal shape functions of the corresponding subdomains in vector form whereas  $N_a$  and  $N_m$  are the number of nodes belonging to each subdomain. Now, the method of weighting residuals is applied to equations (4) and (5) in combination with the Green's theorem and the Galerkin approach [24]. In addition, the rigid wall

boundary condition in the outer surface of the chamber is considered (the normal acoustic velocity being zero) together with the perforated duct impedance  $Z_p$  and the condition of the normal velocity continuity at this surface. The FE equations are

$$\int_{\Omega_a} \nabla^T \mathbf{N}_a \nabla \mathbf{N}_a d\Omega \{ \boldsymbol{\Psi}_a \} + \int_{\Omega_a} (-k_0^2 + 2Mk_0 k_z + (1-M^2)k_z^2) \mathbf{N}_a^T \mathbf{N}_a d\Omega \{ \boldsymbol{\Psi}_a \} = \int_{\Gamma_p} \left( \frac{-j\omega\rho_0 + jMc_0\rho_0 k_z}{Z_p} \right) \mathbf{N}_a^T \mathbf{N}_a d\Gamma \{ \boldsymbol{\Psi}_a \} + \int_{\Gamma_p} \left( \frac{j\omega\rho_0 - jMc_0\rho_0 k_z}{Z_p} \right) \mathbf{N}_a^T \mathbf{N}_m d\Gamma \{ \boldsymbol{\Psi}_m \} + \int_{\Omega_m} \frac{1}{\rho_m} \nabla^T \mathbf{N}_m \nabla \mathbf{N}_m d\Omega \{ \boldsymbol{\Psi}_m \} + \int_{\Omega_m} \frac{1}{\rho_m} (k_z^2 - k_m^2) \mathbf{N}_m^T \mathbf{N}_m d\Omega \{ \boldsymbol{\Psi}_m \} = \int_{\Gamma_p} \frac{j\omega}{Z_p} \mathbf{N}_m^T \mathbf{N}_a d\Gamma \{ \boldsymbol{\Psi}_a \} - \int_{\Gamma_p} \frac{j\omega}{Z_p} \mathbf{N}_m^T \mathbf{N}_m d\Gamma \{ \boldsymbol{\Psi}_m \} \quad , (8)$$

$$\int_{\Gamma_p} \frac{j\omega}{Z_p} \mathbf{N}_m^T \mathbf{N}_a d\Gamma \{ \boldsymbol{\Psi}_a \} - \int_{\Gamma_p} \frac{j\omega}{Z_p} \mathbf{N}_m^T \mathbf{N}_m d\Gamma \{ \boldsymbol{\Psi}_m \} \quad , (9)$$

These equations allow the computation of the wavenumbers and the pressure modes by solving an eigenvalue problem [4].

## 2.3. Continuity of the acoustic fields

Numerical mode matching [6] is applied now by enforcing two conditions over the inlet/outlet planes A and B (see Figure 1). The first condition is given by the continuity of pressure, the incident eigenfunction of the inlet pipe being chosen as weighting function. The second matching condition is a kinematic relation that considers continuity of the axial acoustic velocity, where the incident eigenfunction in the chamber has been chosen as weighting function. The weighted integrals are numerically evaluated after truncating the number of unknown modal amplitudes to  $n$ . Then the equations are solved simultaneously to find the unknown modal amplitudes, after setting the amplitude of the incident wave in the inlet equal to 1 and considering an anechoic termination. Finally, taking into account the plane wave conditions in the inlet/outlet pipes, the transmission loss of the silencer can be obtained as follows

$$TL = -20 \log \left| P_{13}^I \right| \quad . (10)$$

Further details of the approach can be found in reference [6].

### 3. Discussion and results

The geometry of the silencer under study consists of a dissipative configuration with circular cross section, its characteristic dimensions being: radius of the inlet/outlet/perforated ducts  $R_1 = 0.0268$  m, outer radius of the chamber  $R_c = 0.091875$  m; inlet/outlet pipes length  $L_{i,o} = 0.1$  m, and chamber length  $L_c = 0.3$  m. The perforated duct has been defined through the following properties:  $t = 0.001$  m, thickness;  $d_h = 0.0035$  m, hole diameter and  $\sigma = 10$  %, porosity. The geometry is axisymmetric and therefore the mesh used to solve the eigenvalue problem in the cross section is composed by one-dimensional quadratic elements with an approximate size of 0.01 m, which allows the computation of an accurate transmission loss. To model the perforated duct, the impedance formula of Lee and Ih [21] has been considered, taking into account that the surface is backed by a porous media [6, 20]. The absorbent material behaviour has been included by means of a two-parameter characterization similar to the model of Delany and Bazley [25]. Here, the characteristic impedance  $Z_m(r)$  and the wavenumber  $k_m(r)$  are defined as follows

$$Z_m(r) = Z_0 \left( 1 + 0.095(\rho_0 f / R(r))^{-0.669} - j 0.169(\rho_0 f / R(r))^{-0.571} \right), \quad (11)$$

$$k_m(r) = k_0 \left( 1 + 0.201(\rho_0 f / R(r))^{-0.583} - j 0.220(\rho_0 f / R(r))^{-0.585} \right), \quad (12)$$

where  $f$  is the frequency,  $Z_0$  is the characteristic impedance of the air (defined as  $Z_0 = \rho_0 c_0$ ) and  $R(r)$  is the absorbent material resistivity that can be calculated at each integration point of the FE mesh through the Christie's formula [17]:

$$R(T(r)) = R(T_{ref}) \left( \frac{T(r) + 273.15}{T_{ref} + 273.15} \right)^{0.6}, \quad (13)$$

$T_{ref}$  being the reference temperature at which the resistivity is known. In the present study, E glass fibre is considered, having a resistivity reference value  $R_{ref} = 30716$  rayl/m for  $T_{ref} = 25$  °C. Table I shows the values of the temperature considered to obtain the coefficients that define the different temperature fields, defined in this work by means of a quadratic polynomial function  $T(r) = T_0 + T_1 r + T_2 r^2$ . This definition fits satisfactorily the logarithmic function that characterizes heat transfer in a cylindrical duct [26].

#### 3.1. Validation of the method

Figure 2 shows the comparison of the results obtained through the present method and the results computed by using a 3D finite element formulation. In both cases a Mach number  $M = 0.1$

has been considered. In the latter case, the temperature field is defined as  $T(r, z) = T_0 + T_1 z + T_2 r + T_3 z r + T_4 z r^2 + T_5 r^2$ , which allows both axial and radial temperature variations. Therefore, a higher number of points are required for its definition (detailed in Table 1). As can be observed, the results obtained by both methods present an excellent agreement, with undistinguishable attenuation curves. A lower attenuation is obtained as the temperature jump is higher [10]. This can be associated with a saturation effect due to the high resistivity of the E glass fibre, which increases with the average temperature of the chamber.

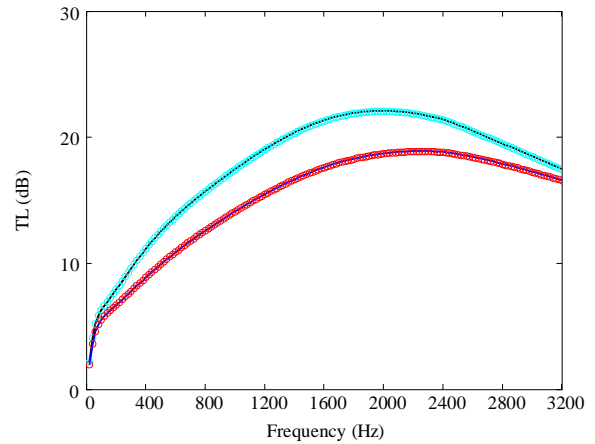


Figure 2. TL of the dissipative silencer with  $M = 0.1$ : —, Case A1, 3D FE formulation; ○○○, same, mode matching; —, Case A2, 3D FE formulation; ○○○, same, mode matching.

#### 3.2. Effect of the radial temperature variation

In this section, a comparison between the results of a full 3D FE model and the numerical mode matching is presented for a Mach number  $M = 0.1$ . The attenuation results have been obtained, on one hand, for temperature distributions that consider axial and radial temperature variations in the silencer (cases B1 and B2 of Table 1), by means of the 3D FE formulation proposed by Denia *et al.* [10]. On the other hand, an approximated temperature distribution has been obtained by averaging the axial thermal gradient while retaining the radial one. This approximation is based on the fact that the influence of the axial variation on the acoustic behaviour of the silencer is lower than the radial effect. The temperature within the duct has been obtained as the average value between the temperatures at the inlet and outlet sections. It has been also considered that in the chamber only radial thermal variation exists. The decrement of the radial temperature in the chamber is equal to

the one considered in the temperature distribution of the full 3D FE model.

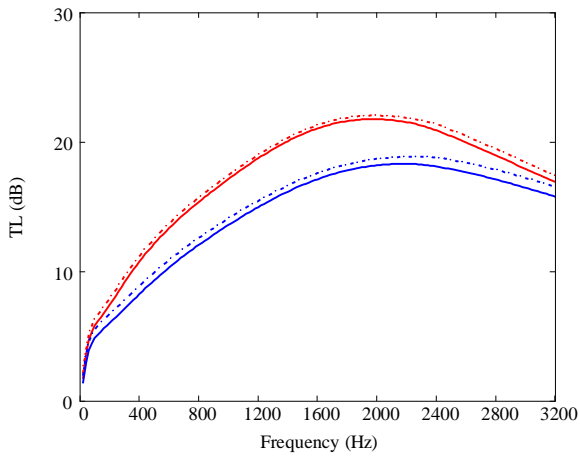


Figure 3. TL of the dissipative silencer with  $M = 0.1$ : - · - · -, Case A1, mode matching; —, Case B1, 3D FE formulation; - · - · -, Case A2, mode matching; —, Case B2, 3D FE formulation.

As can be observed in Figure 3, the attenuation calculated using the approximated temperature distribution provides results quite similar to those obtained with the full 3D FE model, although the TL is slightly overestimated. This overestimation is slightly higher as the radial temperature gradient increases. In the cases under study, the highest TL difference is 5% approximately in the case A2, where the radial variation of the temperature is higher. The computational advantages of the numerical mode matching compared to the 3D full FE approach are, however, quite evident [6], and they are likely to compensate the previous slight TL overestimation in some practical applications.

#### 4. Conclusions

A computationally-efficient numerical technique based on the mode matching method has been developed to study the acoustic behaviour of perforated dissipative silencers of arbitrary cross section with temperature gradients in the absorbent material. The presence of mean flow has been considered in the central duct separated from the

dissipative outer region by a perforated screen. The main advantage of the proposed approach is that strongly reduces the computation time when compared to a full 3D finite element formulation. The technique combines axial and transversal solutions of the wave equation in the different silencer regions. The transversal pressure modes and the corresponding wavenumbers have been obtained by means of a 2D finite element eigenvalue analysis of the cross section, considering a transversal temperature gradient and an adapted version of the wave equation, since the temperature variation leads to non-homogeneous properties of the absorbent material. For the numerical test cases under consideration, the radial temperature gradients have more influence on the acoustic behaviour of the silencer than the axial variations. Thus, an axially uniform temperature field has been considered, its value being the inlet/outlet temperature average, while retaining the transversal gradient in the formulation. In order to keep the numerical efficiency of the approach, the same axial consideration has been applied to the mean flow. Then, considering continuity of the acoustic pressure and axial acoustic velocity fields at the geometrical discontinuities and applying the mode matching method, the modal amplitudes of the waves in the chamber and the inlet/outlet ducts have been obtained. This approach has shown a good agreement with the results achieved by the full 3D finite element technique with less computational effort. In spite of the fact that this method slightly overestimates the attenuation, it is much more efficient from a computational point of view.

Case	Inlet temp. (°C)	Outlet temp. (°C)	Temperature at $R_1$ (°C)	Temperature at mean radius (°C)	Temperature at $R_c$ (°C)
	$T_i$	$T_o$	$T_{int}$ (Inlet/Outlet)	$T_{med}$ (Inlet/Outlet)	$T_{ext}$ (Inlet/Outlet)
A1	250	250	250 / 250	185.48 / 185.48	150 / 150
A2	400	400	400 / 400	270.96 / 270.96	200 / 200
B1	300	200	300 / 200	235.48 / 135.48	200 / 100
B2	500	300	500 / 300	370.96 / 170.96	300 / 100

Table I. Temperature distributions.

## References

- [1] M. L. Munjal. *Acoustics of Ducts and Mufflers*, Wiley, (1987). ISBN 978-0-471-84738-0.
- [2] K. S. Peat, K. L. Rathi. A finite element analysis of the convected acoustic wave motion in dissipative silencers, *Journal of Sound and Vibration*, 184, (1995), 529-545.
- [3] W. Wu, *Boundary Element Acoustics*, WIT Press, Southampton, (2000).
- [4] R. Kirby. Transmission loss predictions for dissipative silencers of arbitrary cross section in the presence of mean flow, *Journal of the Acoustical Society of America*, 114, (2003), 200-209.
- [5] R. Barbieri, N. Barbieri. Finite element acoustic simulation based shape optimization of a muffler, *Applied Acoustics*, 67, (2006), 346-357.
- [6] R. Kirby. A comparison between analytic and numerical methods for modelling automotive dissipative silencers with mean flow. *Journal of Sound and Vibration*, 325, 565-582 (2009).
- [7] F. Piscaglia, A. Montorfano, G. Ferrari, G. Montenegro. High resolution central schemes for multi-dimensional non-linear acoustic simulation of silencers in internal combustion engines, *Mathematical and Computer Modelling*, 54, (2011), 1720-1724
- [8] K. S. Peat, K. L. Rathi. A finite element analysis of the convected acoustic wave motion in dissipative silencers, *Journal of Sound and Vibration*, 184, (1995), 529-545.
- [9] A. G. Antebas, F. D. Denia, A. M. Pedrosa, F. J. Fuenmayor. A finite element approach for the acoustic modeling of perforated dissipative mufflers with non-homogeneous properties. *Mathematical and Computer Modelling*, 57, 1970-1978 (2013).
- [10] F. D. Denia, E. M. Sánchez-Orgaz, J. Martínez-Casas, F. J. Fuenmayor. FE computation of sound attenuation in dissipative silencers with temperature gradients and non-uniform mean flow, 42nd International Congress and Exposition on Noise Control Engineering (Inter-noise), Innsbruck, Austria, (2013).
- [11] R. Glav. The point-matching method on dissipative silencers of arbitrary cross-section, *Journal of Sound and Vibration*, 189, (1996), 123-135.
- [12] R. Glav. The transfer matrix for a dissipative silencer of arbitrary cross-section. *Journal of Sound and Vibration*, 236, (2000), 575-594.
- [13] L. J. Ericsson. Silencers, in: D. E. Baxa (Ed.), *Noise control in Internal Combustion Engines*, Wiley, (1982), 238-292.
- [14] X. Hou, X. Guo, Z. Liu, F. Yan, F. Pen. Flow field analysis and improvement of automobile exhaust system cold end, *International Conference on Computational Intelligence and Software Engineering*, Wuhan, China, (2010).
- [15] Y. H. Kim, J. W. Choi, B. D. Lim. Acoustic characteristics of an expansion chamber with constant mass flow and steady temperature gradient (theory and numerical simulation), *Journal of Vibrations and Acoustics*, 112, (1990), 460-467.
- [16] C. N. Wang, Y. N. Chen, J. Y. Tsai, The application of the boundary element evaluation on a silencer in the presence of a linear temperature gradient, *Applied Acoustics*, 62, (2001), 707-716.
- [17] D. R. A. Christie. Measurement of the acoustic properties of sound absorbing material at high temperatures, *Journal of Sound and Vibration*, 46, (1976), 347-355.
- [18] J. F. Allard, N. Atalla, *Propagation of sound in porous media: Modelling of sound absorbing materials*, Wiley, (2009). ISBN 978-0-470-74661-5.
- [19] P. Williams, R. Kirby, C. Malecki, J. Hill. Measurement of the bulk acoustic properties of fibrous materials at high temperatures, *Applied Acoustics*, 77, (2014), 29-36.
- [20] R. Kirby, A. Cummings. The impedance of perforated plates subjected to grazing gas flow and backed by porous media, *Journal of Sound and Vibration*, 217, (1998), 619-636.
- [21] S. H. Lee, J. G. Ih. Empirical model of the acoustic impedance of a circular orifice in grazing mean flow, *Journal of the Acoustical Society of America*, 114, (2003), 98-113.
- [22] F. P. Mechel. *Formulas of acoustics*, Springer, (2009). ISBN 978-3540425489.
- [23] I. J. Lee and A. Selamet. Measurement of acoustic impedance of perforations in contact with absorbing material in the presence of mean flow, *Noise Control Engineering Journal*, 60, (2012), 258-266.
- [24] O. C. Zienkiewicz, R. L. Taylor, J. Z. Zhu. *The Finite Element Method: Its Basis and Fundamentals*, Elsevier Butterworth-Heinemann, (2005). ISBN 978-1856176330.
- [25] M. E. Delany, E. N. Bazley. Acoustical properties of fibrous absorbent materials, *Applied Acoustics*, 3, (1970), 105-116.
- [26] F. P. Incropera, D. P. Dewitt, T. L. Bergman, A. S. Lavine. *Principles of heat and mass transfer*, Wiley, (2013). ISBN 978-0471457282.